NIH RELAIS Document Delivery

NIH-10286772

JEFFDUYN

NIH -- W1 RA354

JOZEF DUYN
10 Center Dirve
Bldg. 10/Rm.1L07
Bethesda, MD 20892-1150

ATTN:
PHONE: 301-594-7305
FAX: -
E-MAIL:

SUBMITTED: 2002-08-29 17:22:17
PRINTED: 2002-09-03 09:34:02
REQUEST NO.:NIH-10286772
SENT VIA: LOAN DOC
7967408

NIH Fiche to Paper Journal

TITLE: RADIOLOGY
PUBLISHER/PLACE: Radiological Society Of North America Easton Pa
VOLUME/ISSUE/PAGES:1996 Nov;201(2):399-404 399-404
DATE: 1996
AUTHOR OF ARTICLE: Mattay VS; Frank JA; Santha AK; Pekar JJ; Duyn JH; McLaughli
TITLE OF ARTICLE: Whole-brain functional mapping with isotropic MR i
ISSN: 0033-8419
OTHER NOS/LETTERS: Library reports holding volume or year
0401260
8888231
SOURCE: PubMed
CALL NUMBER: W1 RA354
REQUESTER INFO: JEFFDUYN
DELIVERY: E-mail: jhd@helix.nih.gov
REPLY: Mail:

Venkata S. Mattay, MD • Joseph A. Frank, MD • Attanagoda K. S. Santha, PhD • James J. Pekar, PhD
Jeff H. Duyn, PhD • Alan C. McLaughlin, PhD • Daniel R. Weinberger, MD

Whole-Brain Functional Mapping with Isotropic MR Imaging[1]

PURPOSE: **To assess the reliability and sensitivity of gradient-echo, isotropic multisection echo-planar magnetic resonance (MR) imaging for within-subject whole-brain mapping.**

MATERIALS AND METHODS: **Eight right-handed healthy volunteers underwent gradient-echo, echo-planar MR imaging while they performed a motor task on three occasions over 2–3 months. Ninety-six whole-brain volumes were acquired in 8 minutes 48 seconds. A rigorous statistical threshold for determining activation was set at $P < .05$ and was Bonferroni corrected for approximately 15,000 cortical voxels.**

RESULTS: **In all subjects, reproducible activation was demonstrated in multiple cortical areas and in the cerebellum specific to the motor system. Of the activated voxels, 75%–78% were confined to the motor areas during all sessions. No statistically significant difference was found in the proportion of activated voxels in any motor region (relative to the total number of activated voxels in the whole brain) across the three sessions. The centers of mass of the activated areas were within 2.5 resolution elements of the image across the three sessions.**

CONCLUSION: **Isotropic multisection echo-planar MR imaging has the potential for noninvasive, reliable within-subject mapping of whole-brain functional anatomy.**

HUMAN brain mapping is an important clinical and research approach to understanding functional neuroanatomy. Brain mapping has developed substantially from attempts that were based on clinical-pathologic correlations and invasive cortical stimulation techniques to noninvasive functional magnetic resonance (MR) imaging. Whole-brain mapping has been performed primarily with nuclear medicine techniques, which in general have necessitated intersubject averaging, and thus provide information only about tendencies in groups of people to use brain systems that serve certain behaviors.

Of the currently available approaches, only functional MR imaging based on blood oxygenation level dependent (BOLD) contrast (1,2) has the potential for widespread application because it is noninvasive, has superior spatial and temporal resolution, does not involve radiation exposure, and can be performed with widely available MR instruments. These advantages enable the unique capability of performing repeated within-subject mapping, which is necessary to study individual variability associated with learning and neural plasticity. Previous reports in which the application of functional MR imaging to brain mapping was demonstrated (3–8), however, have been limited because the whole brain was not covered. In addition, the reliability and sensitivity of these methods have not been subjected to rigorous evaluation, which is essential before studies can be undertaken of learning, memory, and other complex aspects of human functional neuroplasticity.

Whole-brain methods are essential to map complex behaviors because such behaviors involve distributed neural components. Furthermore, whole-brain methods facilitate registration of each functional volume to one another, permitting correction for subject motion during imaging, an important step in data processing. In functional MR imaging techniques in which only a fraction of the brain is surveyed, motion correction is difficult. A whole-brain method with isotropic resolution would have the additional features of permitting resectioning of the final data in any arbitary geometry with minimal interpolation errors and of facilitating more accurate anatomic localization.

In this study, we performed whole-brain BOLD functional MR imaging with interleaved sagittal isotropic multisection echo-planar imaging in healthy volunteers while they per-

Index terms: Brain, function, 13.92 • Brain, MR, 13.121412 • Magnetic resonance (MR), brain mapping, 13.12142 • Magnetic resonance (MR), technology, 13.121412

Abbreviations: BOLD = blood oxygenation level dependent, CER = right cerebellum, PAR = parietal cortex, PM = lateral premotor area, PSM = primary sensorimotor cortex, SMA = supplementary motor area, VOI = volume of interest.

Radiology 1996; 201:399–404

[1] From the Clinical Brain Disorders Branch, National Institutes of Health, National Institute of Mental Health Neuroscience Center at St Elizabeth's, 2700 Martin Luther King Jr Ave SE, Washington, DC 20032 (V.S.M., A.K.S.S., A.C.M., D.R.W.); the Laboratory of Diagnostic Radiology Research, Office of Intramural Research, National Institutes of Health, Bethesda, Md (V.S.M., J.A.F., J.H.D.); and the Institute for Cognitive and Computational Sciences, Georgetown University Medical Center, Washington, DC (J.J.P.). Received April 1, 1996; revision requested May 22; revision received June 18; accepted June 24. **Address reprint requests to** D.R.W.

formed a simple overlearned motor task. We describe the regional specificity, sensitivity, and reliability of the activation maps.

MATERIALS AND METHODS

Data Acquisition

Imaging was performed with a 1.5-T Signa MR imager (GE Medical Systems, Milwaukee, Wis) equipped with a combined radio-frequency and gradient insert coil capable of generating 2 G/cm (0.0002 T/cm) with a rise time of 100 μsec (Medical Advances, Milwaukee, Wis). Foam padding was used to limit head motion within the coil. The protocol was approved by the intramural review board of the National Institute of Mental Health.

After a T1-weighted spin-echo axial localizing image was obtained (repetition time, 400 msec; echo time, 10 msec; [400/10]; flip angle, 90°; section thickness, 5 mm; field of view, 30 cm; matrix, 256 × 128), 56 sagittal (3.75 mm thick) interleaved sections were acquired with gradient-echo echo-planar imaging (field of view, 24 cm; matrix, 64 × 64; 5,500/60; flip angle, 90°), which provided air-to-air coverage. This high-duty cycle (56 sections every 5,500 msec) was achieved without an increase in temperature of the insert coil above manufacturer specifications. Shimming was performed over the whole brain with the autoshim feature, and additional manual adjustments were based on the peak height of the water signal. Fifty-six T1-weighted, spin-echo, sagittal anatomic images (section thickness, 3.75 mm; field of view, 240 mm; matrix, 256 × 256; 500/10; flip angle, 90°) were also obtained in 4 minutes 66 seconds.

Subjects and Task

The study was approved for human subjects by the intramural research review board of the National Institute of Mental Health, National Institutes of Health. Eight healthy volunteers (three men and five women; mean age, 30 years; range, 23–37 years) gave written informed consent after the nature and possible adverse effects of the procedure were explained. All subjects were strongly right handed according to the Edinburgh Handedness Inventory (mean score, 91) (9). The subjects were requested to abstain from nicotine and caffeine for 4 hours and from over-the-counter medications for 24 hours before the imaging sessions.

Images were obtained while subjects performed a motor task with the right hand. Subjects opposed the thumb to the tips of the other four fingers in a sequential manner (1,2,3,4, 1,2,3,4, and so on) at a rate of about 2 Hz (self paced). To establish the reliability of the method, subjects repeated the study two additional times at 4–8-week intervals. The motor task was performed under the same conditions at all three sessions. To avoid a practice or learning effect, the subjects practiced the task before the imaging session on each day.

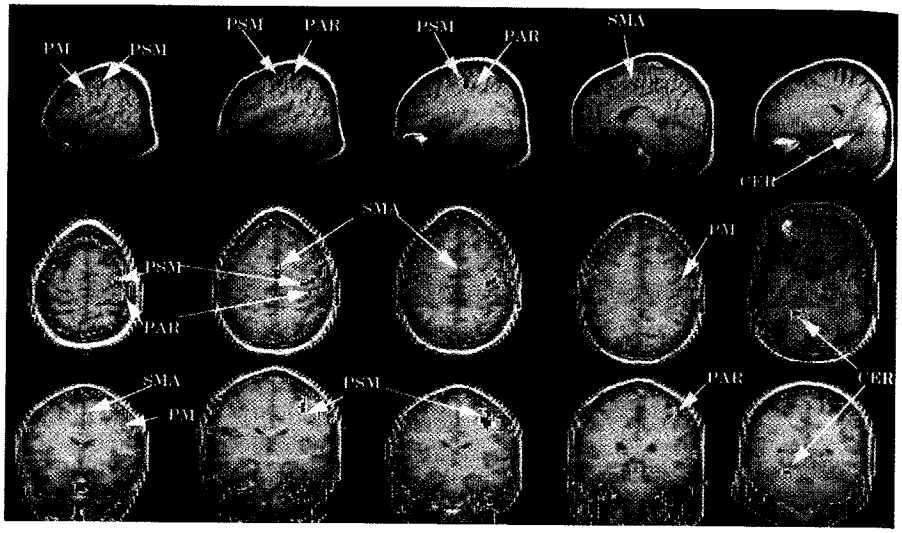

Figure 1. Selected sagittal, axial, and coronal sections of functional data from one trial in one subject are mapped onto a high-resolution, T1-weighted MR image. Red voxels represent those that surpass the critical *t* statistical threshold and are defined as activated. Images display the region-specific distribution of the activated voxels in the left PSM, left PM, left PAR, left SMA, and right CER.

The stimulation protocol consisted of 16 33-second epochs (eight off-on cycles), alternating a rest (off) state with a motor sequence (on) state. Ninety-six whole-brain multisection echo-planar volumes were acquired in 8 minutes 48 seconds (5.5 seconds per one whole brain acquisition and six acquisitions for each off or for each on state).

Analysis of Time Series Data

Image reconstruction and subsequent analysis of the time course data were performed off line. A threshold signal intensity (noise threshold) for excluding voxels outside the brain was estimated by using a histogram of the signal intensities of all the voxels. Voxels with a signal intensity below the noise threshold were excluded. To minimize motion artifacts, each three-dimensional brain volume was registered to the first in the time series with the automated image registration program (10). BOLD responses have an inherent delay of about 4–6 seconds (11). To control for this delay, the first brain volume of each state (on and off) was excluded from further analysis. The last brain volume of each state was also excluded from further analysis because of the uncertainty of the exact end and start of neighboring on and off states. This reduced the total number of brain volumes acquired in a study to 64.

A voxel-wise review of the time course data revealed random low-frequency drifts (~2 cycles per the entire 8 minutes 48 seconds of data acquisition) in the baselines of many voxels, with a maximum amplitude of approximately 5% of the baseline signal intensity. To remove potential artifacts from these low-frequency oscillations, the signal intensities of each voxel (ie, the time course data) were fitted to a third-degree polynomial with time as the independent variable. The time-dependent terms of the polynomial fit were subtracted from the time course data on a voxel-by-voxel basis. From the corrected time course data, the mean signal intensity and standard error were determined for the on and off states for each voxel. From these data, a voxel-wise variance term (denominator in the *t* statistic) was derived as follows:

$$\sigma_{\bar{x}_{on}-\bar{x}_{off}} = \sqrt{[(\sigma^2_{on}/N_{on}) + (\sigma^2_{off}/N_{off})]},$$

where $\bar{x}_{on}$ = mean voxel signal intensity from all the time points in the on states, $\bar{x}_{off}$ = mean voxel signal intensity from all the time points in the off states, σ_{on} = standard deviation of voxel signal intensity in the on states, σ_{off} = standard deviation of voxel signal intensity in the off states, N_{on} = number of time points in the on state, and N_{off} = number of time points in the off state.

Whole-brain histograms of these variances had abnormally long tails and did not conform to a χ^2 distribution. This precluded the assumption of a homogeneous variance across the image; therefore, a Student *t* test (which uses the individual voxel variance) rather than a *z* statistic (which uses a pooled variance) was used to identify voxels with a statistically significant difference in mean signal intensity between the on and off states (12). By using a previously described method (12,13), the effective degrees of freedom to define the null distribution of the *t* values was calculated to be 48. Since brain cortex represents approximately 50%–60% of total brain volume (14), under the assumption that the voxels represent independent resolution elements, an unbiased Bonferroni correction (one-sided probability of 0.025) for approximately 15,000 contrasts in the brain cortex (60% of ~25,000 voxels in the whole brain) was used to establish a rigorous statistical threshold. The one-

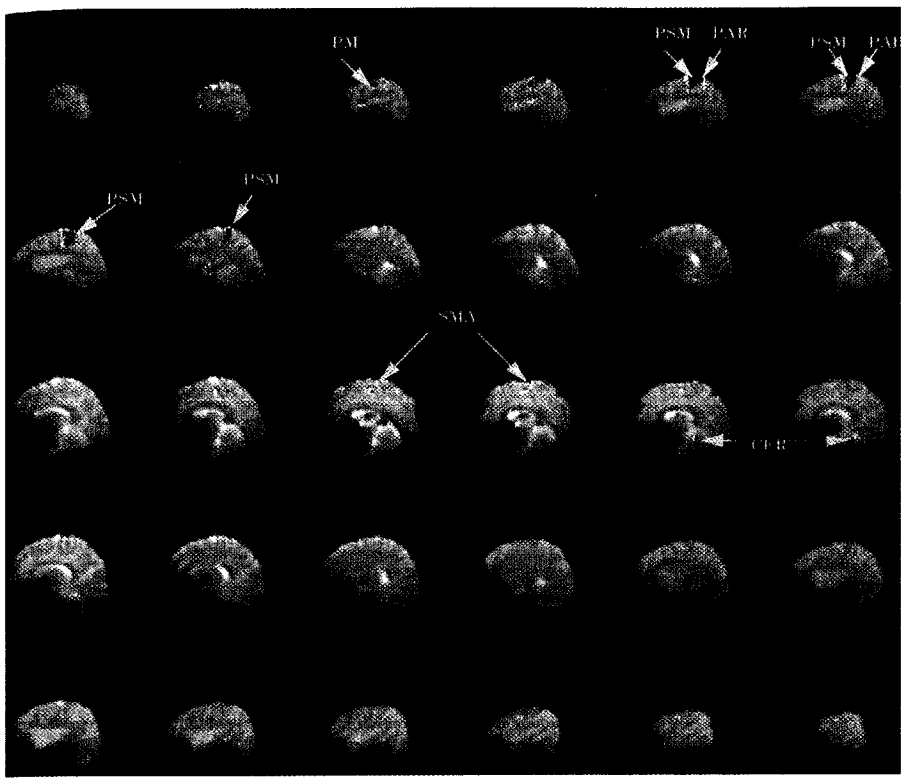

a.

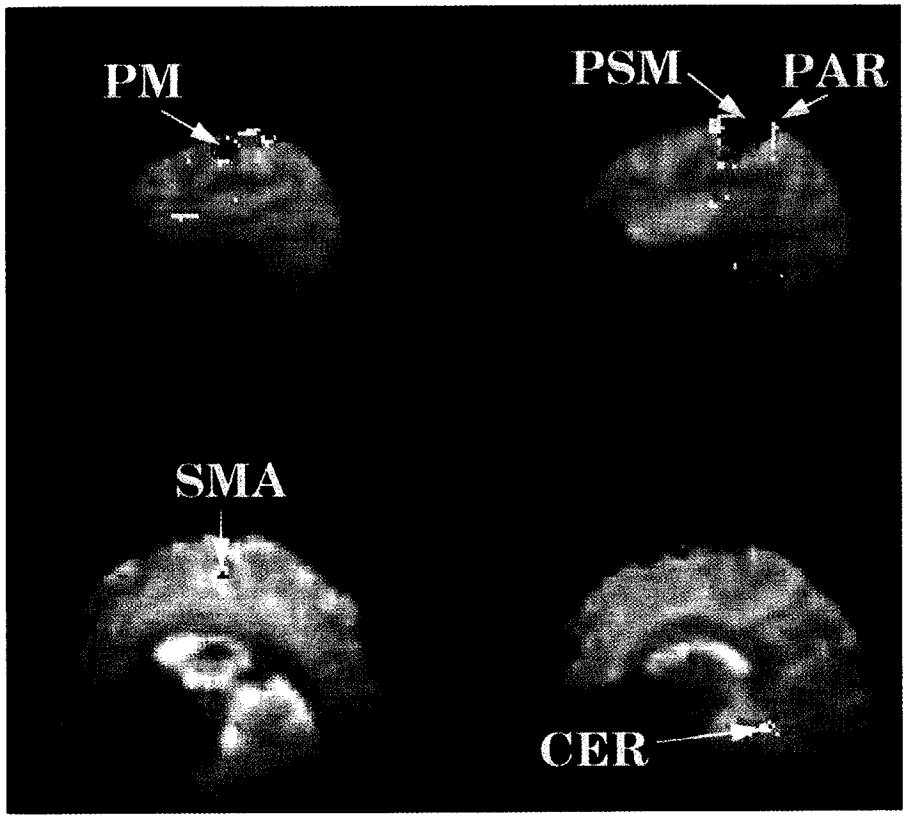

b.

Figure 2. **(a)** Activated voxels in the various motor regions from all three sessions in one subject are overlaid on sagittal echo-planar images. Colored regions represent activated voxels (blue = day 1, green = day 2, yellow = day 3). Red regions represent activated voxels that were common to all three sessions. **(b)** Magnified views of sections 3, 5, 15, and 17 show the overlapping voxels in the various motor regions.

sided probability of 0.025 becomes approximately 0.017×10^{-4} when Bonferroni corrected (0.025 divided by ~15,000 contrasts). The corresponding t cutoff was approximately 5.25 (varying slightly from subject to subject), and voxels above this threshold were considered activated.

Maps of activated voxels were created for qualitative and quantitative analysis.

Comparisons between Sessions

For each subject, the 64 functional brain volumes from day 1 and day 3 were registered to the brain volumes from day 2 by using the automated image registration program (10). Regions of interest were then drawn on sagittal sections of the high-resolution anatomic image from day 2 for each of the motor regions on the basis of standard anatomic atlases (15). The extent of the motor regions of interest was defined as follows: (*a*) the primary sensorimotor cortex (PSM), which was the area that encompassed the central sulcus, including the posterior half of the precentral gyrus and the anterior half of the postcentral gyrus; (*b*) the lateral premotor region (PM), which was the area that encompassed the precentral sulcus, including the anterior half of the precentral gyrus; (*c*) the parietal region (PAR), which was the area that encompassed the postcentral sulcus, the posterior half of the postcentral gyrus, and the area posterior to the postcentral sulcus; (*d*) the supplementary motor area (SMA), which was the area anterior to the mesial aspect of the precentral gyrus; and (*e*) the ipsilateral cerebellum, which was the area that encompassed the superior half of the right cerebellum (CER). Regions of interest that represented a specific motor area from many sections were then combined to define a three-dimensional volume of interest (VOI). These three-dimensional VOIs were then applied to the t maps. The same VOIs were applied for all three sessions.

Stringent criteria were used to define activation; thus, for each motor region, the smallest number of activated voxels from any of the three sessions was considered to represent the principal focus of activation and was defined as the core activated area for that region. Additional measurements obtained in each VOI were (*a*) the number of activated voxels, (*b*) the mean percentage signal intensity change in the activated voxels, (*c*) the relative proportion of activated voxels in each motor region, (*d*) the absolute distance between the centers of mass of the cluster of activated voxels in each motor region across the three trials, (*e*) the number of voxels in the core activated area of each motor region that were reliably activated in all three sessions, and (*f*) the "false-alarm" rate.

The relative proportion of activated voxels in each motor region was calculated by dividing the number of activated voxels in each region by the number of activated voxels in the whole brain. The absolute distance between the centers of mass of each of the clusters of activated voxels in the various motor regions during the three sessions was determined by first calculating the t-weighted center of mass

Absolute Three-dimensional Distance in Voxels between the Center of Mass for Each of the Clusters of Activated Voxels in the Various Motor Regions across the Three Trials

Subject	PSM	SMA	CER	PM	PAR
1	0.38	0.69	0.68	...	1.12
2	0.67	0.71	1.64	0.52	1.09
3	0.58	0.94	2.12	1.65	2.50
4	0.95	1.17	1.20	3.21	0.76
5	0.23	0.72	2.32	0.66	1.42
6	1.16	2.30	1.26	1.73	1.76
7	0.36	1.08	0.44	3.61	0.82
8	1.41	0.70	1.19	5.90	0.94
Mean	0.72	1.04	1.35	2.47	1.30
SD	0.42	0.54	0.75	1.91	0.58

Note.—SD = standard deviation.

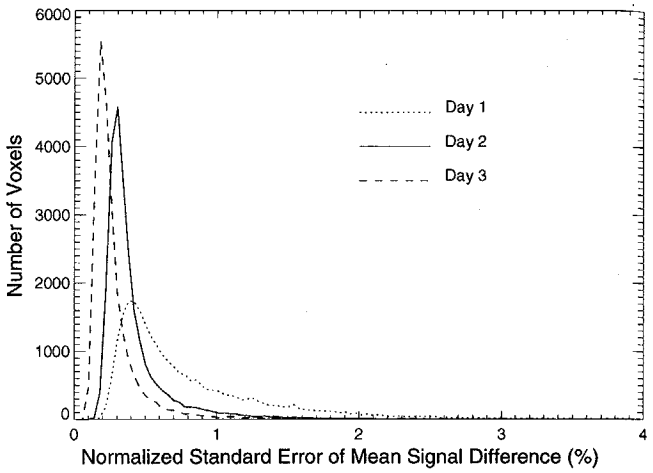

Figure 3. Histograms show standard errors of differences in voxel signal intensity (on states minus off states) for all three sessions in one subject.

(in arbitrary x, y, and z coordinates) of the cluster of activated voxels for each region. The absolute distance in number of voxels in three-dimensional space between the centers of mass for each region between day 1 and day 2, day 2 and day 3, and day 1 and day 3 was then calculated, and the mean value of these three measurements was considered the distance in voxels between the center of mass of each cluster across the three sessions. To identify specific voxels that were activated in all three sessions, the x, y, and z coordinates of each voxel in the core-activated area for each motor region were determined. The number of activated voxels in these core areas that was common to all 3 days was then calculated and expressed as a percentage of the total number of voxels in the core activated area.

To establish that activated voxels shared across the 3 days were not due to chance, VOIs the same size as the VOI with the least reliable proportion of shared voxels in a core-activated area (the PM in this study) were placed in 10 locations outside the motor regions. A series of χ^2 analyses was performed to compare the proportion of shared activated voxels in the PM with that in each of the 10 control VOIs. The false-alarm rate was calculated by dividing the number of voxels outside the motor areas that were classified as activated in all three sessions by the total number of cortical voxels in the whole brain, excluding the motor VOIs.

A one-way analysis of variance with time as a repeated measurement was used to compare the number of activated voxels in the whole brain across the three sessions. Analysis of variance was also used to compare the following measures in each motor region across the three sessions: (*a*) the mean number of activated voxels, (*b*) the mean percentage signal intensity change in the activated voxels, and (*c*) the relative proportion of activated voxels (relative to the total number of activated voxels in the whole brain). For each motor region, the number of activated voxels in the VOI and the number of activated voxels in the whole brain were examined with linear regression analysis. This involved 24 points for each region (eight subjects × three sessions). Finally, histograms of the voxel variances from the three sessions were plotted and compared.

RESULTS

All subjects showed activation in the left PSM, left SMA, and left PAR in all test sessions. Seven of the eight subjects also showed activation in the left PM and right CER on all three occasions. The foci of activation are shown in Figure 1. In one subject, the cerebellum was inadvertently not included in the field of view on day 1. In this subject, activation was seen in the ipsilateral cerebellum on days 2 and 3, when an appropriate field of view was used. Overall, about 1% of the total number of voxels in the whole brain (mean, 24,650 voxels) surpassed the statistical threshold of significance and were considered activated. Of the activated voxels, 75%–78% were located in the contralateral cortical motor areas (PSM, SMA, PAR, and PM) and ipsilateral cerebellum in each of the three sessions (Fig 2). No activated voxels were seen overlying the noncortical regions of the brain (eg, ventricular cerebrospinal fluid space and white matter regions, such as centrum semiovale). Mean (plus or minus standard error) percentage changes in signal intensity over the three sessions in the activated voxels were as follows: PSM = 2.35% ± 0.08, SMA = 1.82% ± 0.13, PAR = 2.13% ± 0.10, PM = 1.95% ± 0.14, and CER = 1.77% ± 0.14.

Even though the absolute number of activated voxels in a region and in the whole brain varied to some degree across the three sessions (PSM: $F = 3.16$, $P < .07$), a one-way analysis of variance with time as a repeated measure did not reveal statistically significant differences in the proportion of activated voxels (relative to the total number of activated voxels in the whole brain) in any motor region across the three sessions ($P > .25$). The mean percentage change in signal intensity in the activated voxels in each motor region also varied to some degree across the three sessions.

The mean distance between the centers of mass of the activated motor areas ranged between 0.72 voxels for PSM and 2.47 voxels for PM across the three sessions (Table). The mean percentage of voxels in the core activated areas that reliably superseded the threshold in all three sessions were as follows: PSM, 70%; SMA, 60%; CER, 55%; PM, 22%; and PAR, 44%. One subject did not show activated voxels that were common to all three sessions in the CER. Similarly, although there were activated voxels in the left PM region in seven of the eight subjects on all 3 days, three subjects did not show activated voxels that were common to all three sessions in this region. The series of χ^2 analyses, in which motor and nonmotor VOIs were compared, revealed that the probability of voxels in the core activated areas (including the PM region) being activated on all 3 days as a chance occurrence was low ($P < 1.0 \times 10^{-6}$).

The false alarm rate in the nonmotor cortical regions was 0.0002. Results of χ^2 analysis revealed that this frequency was significantly lower ($P < 1.0 \times 10^{-6}$) than that of activated voxels shared across the three sessions, even in the VOI with the least reliable proportion of the core activated area (PM in this study).

Correlations between the total and

regional number of activated voxels for all subjects across all trials were high (r = .88 for PSM, .82 for PM, .85 for SMA, .86 for PAR, and .75 for CER; $P < .01$). Histograms of standard errors of differences in individual voxel signal intensity over time showed that the plots varied from one trial to another in every subject (Fig 3). There did not appear to be any systematic pattern as to which imaging session showed the most voxel-wise variance.

DISCUSSION

BOLD functional MR imaging has the unique capability of within-subject brain mapping, as illustrated by several reports in the literature of functional MR imaging performed during motor tasks. However, these earlier studies were based on techniques that survey only a limited span of the brain (4,6,8,16,17), thus failing to document the distributed components of the map. In our study, we describe a BOLD functional MR imaging method that is capable of isotropic whole-brain coverage. With this method, reliable and region-specific activation was seen in all cortical motor areas, as well as in the ipsilateral cerebellum within individual subjects in all three sessions. The isotropic acquisition is advantageous for resectioning of data in coronal and axial planes and for more accurate anatomic localization. To our knowledge, this is the first study to map distributed activation sites in the motor system at multiple levels of the neuraxis in individual subjects.

Although BOLD signals may be confounded by variables such as draining veins and inflow (18), the contribution from inflow to echo-planar data with a repetition time greater than 2 seconds is probably small (19). Further, the geometry of the blood vessels is likely to be a more important factor in images acquired in the axial plane. The profile of vessels in the acquired voxel is probably much smaller in sagittal acquisitions, and use of an interleaved method further minimizes these artifacts. Sagittal acquisition also enables whole-brain coverage with a smaller field of view than that required for whole-brain coverage in the axial dimension.

Earlier brain mapping studies have established that even the simplest motor behaviors involve the joint operation of many neural components (20–25). The principal cortical components of the motor system include the contralateral PSM (Brodman areas 1, 2, 3, and 4), SMA (Brodman area 6), PM (Brodman area 6), PAR (Brodman areas 5 and 7), and ipsilateral cerebellum. Although some positron emission tomographic studies (23,26–29) have shown activation in all these areas, most of these were studies of groups of subjects in which data were averaged together. It has not been clear how representative the pattern is of every individual subject.

In our study, all subjects showed activation (as defined by voxels that surpassed a rigorous statistical threshold of significance) in the left PSM, left SMA, and left PAR at all test sessions. Seven of the eight subjects also showed activation in the left PM and in the right CER on all three occasions. Absence of lateral premotor activation in one subject on all 3 days may reflect an individual variation in cortical representation of the motor system. Reproducible ipsilateral cerebellar activation was seen in all but one subject in whom the cerebellar region was inadvertently not included in the field of view on day 1. Proper care was taken to ensure that this subject was placed farther into the gantry during the repeat studies, and activation was seen in the ipsilateral cerebellum on days 2 and 3.

The regional specificity of the activation to the motor system is highlighted by the finding that the greatest portion (75%–78%) of voxels that surpassed the statistical threshold of significance were located in the contralateral cortical motor areas (PSM, SMA, PAR, and PM) and ipsilateral cerebellum (Figs 1, 2). Areas of activation were also seen in the anterior cingulate, right SMA, right PM, right PSM, right PAR, and temporal and prefrontal regions. Activation of these areas was not consistent in all subjects or even within subjects at repeat trials. On average, only two voxels in the entire expanse of nonmotor brain regions showed activation on all 3 days. Because a stringent statistical thresholding procedure was used, it is unlikely that activated voxels in these nonmotor areas are products of random noise. Rather, they may reflect individual variability in brain function related to motor activity and/or cortical processing, related to idiosyncratic, nonmotor aspects of the repetitive task.

The regional specificity of the activation maps is further established by the lack of activated voxels in non–gray matter areas of the brain. Statistically significant activation was not seen in the basal ganglia in any subject. Even though some positron emission tomographic studies (30–32) have shown activation in the basal ganglia during similar motor tasks, these results were based on intersubject averaging of groups and not on individual subjects. Furthermore, positron emission tomographic studies (32,33) during motor tasks have shown that the signal intensity changes in the basal ganglia are smaller than those seen in cortical motor areas, which may explain the lack of statistically significant activation according to our stringent criteria in basal ganglia in individual subjects.

We examined the reliability of the activation responses across the 3 days in terms of several parameters: variation in the number of activated voxels, the proportion of activated voxels (relative to the total number of activated voxels in the whole brain), the mean percentage change in signal intensity of the activated voxels, the distance between the t-weighted centers of mass of the activated voxels in each motor region, the proportion of voxels in the core activated area that were reliably activated on all three sessions, and the false alarm rate. Despite the reproducibility of the activation of all the contralateral cortical motor areas and ipsilateral cerebellum, the exact size of the activated area in these areas varied between and within subjects from session to session. The total number of activated voxels and mean percentage change in signal intensity in each session was also variable. Histograms of individual voxel variances revealed that the plots varied nonsystematically from one trial to another in the same subject (Fig 3). This variation in voxel variances most likely accounts for some of the variations in the absolute number of activated voxels from one day to another. To our knowledge, the distribution of the stability of voxel signal intensity across time has not been evaluated in previous functional MR studies and may affect the interpretation of serially performed studies.

Fluctuations of voxel variances across different sessions in the same subject may be due to a number of factors, including technical factors such as motion (during imaging), physiologic factors such as heart rate and respiratory rate, and psychological factors such as attention and arousal. Variance, a key element in the estimation of the voxel t value, can be high or low depending on the effect of such factors. Motion is very likely to increase variance. Unstable voxels can thus not make the critical t threshold, resulting in fewer activated

voxels in a study. Therefore, to use imaging techniques effectively in longitudinal studies or for comparison of healthy subjects with patients who have brain disorders, it is crucial to minimize motion to optimize the stability of the technique and obtain comparable parameters across studies. Motion-detecting algorithms and near-real-time analysis and display of functional MR images will help achieve this goal (34). Real-time functional MR imaging enables adjustments to be made while the subject is still in the imaging unit, to optimize signal stability across sessions and also to correct artifacts, such as from stimulus-correlated motion. This can enable investigators to reacquire data in the same session after making the necessary adjustments.

It is important to note that, although the total number of activated voxels varied from session to session, the proportion of activated voxels in the various cortical regions specific to the motor system remained fairly constant and did not significantly differ in any region across the three sessions. These results indicate that the sensitivity of the method to region-specific activation is reproducible at least in terms of the relative focality of the signal intensity changes. In addition, the centers of mass of the activated areas within the motor regions were, on average, within only 1.0–2.5 resolution elements of the image across the three trials (Table). In all these areas, the voxels that were common to all three sesssions in the core activated areas were reproduced with fair reliability (PSM, 70%; SMA, 60%; CER, 55%; PM, 22%; and PAR, 44%). These results further indicate that the principal focus of activation in the various motor areas was reliably localized. We found that the probability of this localization occurring by chance, even in the least reliable region (PM), is small ($P < 1.0 \times 10^{-6}$).

To our knowledge, this is the first functional MR imaging study to demonstrate reliable activation in the cerebellum concomitant with activation in the PSM and other nonprimary cortical motor areas in a single study. The 0.05-mL resolution of this method is superior to the spatial resolution of whole-brain mapping methods in which ionizing radiation is used. In addition, our study illustrates some technical issues that may affect the analysis and interpretation of data related to longitudinal studies. We believe that this approach represents a step forward in the search for a whole-brain mapping functional MR imaging method with a high level of functional-anatomic correlation, as well as statistical power and reliability. ■

Acknowledgments: We thank the following individuals for invaluable technical assistance: Eric C. Wong, MD, PhD, Peter Jezzard, PhD, Roger Woods, MD, John Ostuni, PhD, Roy Sexton, BA, Kathleen Tallent, BS, and Claire de Neree tot Babberich. We also thank Richard Coppola, PhD, and Terry Goldberg, PhD, for helpful suggestions about data analysis. This work was performed in the In Vivo NMR Research Center at the National Institutes of Health.

References

1. Kwong KK, Belliveau JW, Chesler DA, et al. Dynamic magnetic resonance imaging of human brain activity during primary sensory stimulation. Proc Natl Acad Sci USA 1992; 89:5675–5679.
2. Ogawa S, Tank DW, Menon R, et al. Intrinsic signal changes accompanying sensory stimulation: functional brain mapping with magnetic resonance imaging. Proc Natl Acad Sci USA 1992; 89:5951–5955.
3. Kim SG, Ashe J, Georgopoulos AP, et al. Functional imaging of human motor cortex at high magnetic field. J Neurophysiol 1993; 69:297–302.
4. Kim SG, Ugurbil K, Strick PL. Activation of a cerebellar output nucleus during cognitive processing. Science 1994; 265:949–951.
5. Rao SM, Binder JR, Bandettini PA, et al. Functional magnetic resonance imaging of complex human movements. Neurology 1993; 43:2311–2318.
6. Rao SM, Binder JR, Hammeke TA, et al. Somatotopic mapping of the human primary motor cortex with functional magnetic resonance imaging. Neurology 1995; 45:919–924.
7. Duyn JH, Mattay VS, Sexton RH, et al. 3-dimensional functional imaging of human brain using echo-shifted FLASH MRI. Magn Reson Med 1994; 32:150–155. [Erratum: Magn Reson Med 1994; 32:545.]
8. Van Gelderen P, Ramsey NF, Liu G, et al. Three-dimensional functional magnetic resonance imaging of human brain on a clinical 1.5-T scanner. Proc Natl Acad Sci USA 1995; 92:6906–6910.
9. Oldfield RC. The assessment and analysis of handedness: the Edinburgh inventory. Neuropsychologia 1971; 9:97–113.
10. Woods RP, Cherry SR, Mazziotta JC. Rapid automated algorithm for aligning and reslicing PET images. J Comput Assist Tomogr 1992; 16:620–633.
11. Ogawa S, Menon RS, Tank DW, et al. Functional brain mapping by blood oxygenation level-dependent contrast magnetic resonance imaging: a comparison of signal characteristics with a biophysical model. Biophys J 1993; 64:803–812.
12. Worsley K, Friston K. Analysis of fMRI time-series revisited: again. Neuroimage 1995; 2:173–181.
13. Friston K, Holmes A, Poline J, et al. Analysis of fMRI time-series revisited. Neuroimage 1995; 2:45–53.
14. Ziles K. Cortex. In: Paxinos G, ed. The human nervous system. San Diego, Calif: Academic Press, 1990; 757–760.
15. Talairach J, Tournoux P, eds. Referentially oriented cerebral MRI anatomy. New York, NY: Thieme, 1993.
16. Sanes JN, Donoghue JP, Thangaraj V, Edelman RR, Warach S. Shared neural substrates controlling hand movements in human cortex. Science 1995; 268:1775–1777.
17. Karni A, Meyer G, Jezzard P, Adams MM, Turner R, Ungerleider LG. Functional MRI evidence for adult motor cortex plasticity during motor skill learning. Nature 1995; 377:155–158.
18. Duyn JH, Moonen CT, vanYperen GH, deBoer RW, Luyten PR. Inflow versus deoxyhemoglobin effects in BOLD functional MRI using gradient echoes at 1.5 T. NMR Biomed 1994; 7:83–88.
19. Duyn JH. Effects of large vessels in functional magnetic resonance imaging at 1.5 T. Int J Imaging Sys Technol 1995; 6:245–252.
20. Powell TPS, Mountcastle VB. The cytoarchitecture of the postcentral gyrus of the monkey Macaca mulatta. Bull John Hopkins Hosp 1959; 105:108–131.
21. Jones EG, Coulter JD, Hendry SHC. Intracortical connectivity of architectonic fields in the somatic, sensory, motor and parietal cortex of monkeys. J Comp Neurol 1978; 181:291–348.
22. Soso MJ, Fetz EE. Responses of identified cells in postcentral cortex of awake monkeys during comparable active and passive joint movements. J Neurophysiol 1980; 43: 1090–1110.
23. Fox PT, Fox JM, Raichle ME, Burde RM. The role of cerebral cortex in the generation of voluntary saccades: a positron emission tomographic study. J Neurophysiol 1985; 54:348–369.
24. Mountcastle VB. The world around us: neuronal command functions for selective attention. Neurosci Res Prog Bull 1976; 14: 1–47.
25. Ito M. The cerebellum and neural control. New York, NY: Raven, 1984.
26. Fox PT, Raichle ME, Thach WT. Functional mapping of the human cerebellum with positron emission tomography. Proc Natl Acad Sci USA 1985; 82:7462–7466.
27. Colebatch JG, Deiber MP, Passingham RE, Friston KJ, Frackowiak RSJ. Regional cerebral blood flow during voluntary arm and hand movements in human subjects. J Neurophysiol 1991; 65:1392–1401.
28. Deiber MP, Passingham RE, Colebatch JG, Friston KJ, Nixon PD, Frackowiak RSJ. Cortical areas and the selection of movement: a study with positron emission tomography. Exp Brain Res 1991; 84:393–402.
29. Remy P, Zilbovicius M, Leroy-Willig A, Syrota A, Samson Y. Movement and task-related activations of motor cortical areas: a positron emission tomographic study. Ann Neurol 1994; 36:19–26.
30. Seitz RJ, Roland PE, Bohm C, Grietz T, Stone-Elander S. Motor learning in man: a positron emission tomographic study. Neuroreport 1990; 1:17–20.
31. Shibaski H, Sadato N, Lyshkow H, et al. Both primary motor cortex and supplementary motor area play an important role in complex finger movement. Brain 1993; 116:1387–1398.
32. Jenkins IH, Brooks DJ, Nixon PD, Frackowiak RSJ, Passingham RE. Motor sequence learning: a study with positron emission tomography. J Neurosci 1994; 14: 3775–3790.
33. Sadato N, Zeffiro TA, Campbell G, Konishi J, Shibaski H, Hallett M. Regional cerebral blood flow changes in motor cortical areas after transient anesthesia of the forearm. Ann Neurol 1995; 37:74–81.
34. Cox RW, Jesmanowicz A, Hyde JS. Real-time functional magnetic resonance imaging. Magn Reson Med 1995; 33:230–236.